

Concomitant but disappearing: two polymorphs of 1,4-bis(tribromomethyl)benzene

Peter G. Jones,^{a*} Henning Hopf,^b Anamaria Silaghi^b and Christian Näther^c

^aInstitut für Anorganische und Analytische Chemie, Technische Universität Braunschweig, Postfach 3329, 38023 Braunschweig, Germany, ^bInstitut für Organische Chemie, Technische Universität Braunschweig, Postfach 3329, 38023 Braunschweig, Germany, and ^cInstitut für Anorganische Chemie, Christian-Albrechts-Universität zu Kiel, Otto-Hahn-Platz 6/7, 24098 Kiel, Germany
Correspondence e-mail: p.jones@tu-bs.de

Received 14 September 2011

Accepted 16 September 2011

Online 28 September 2011

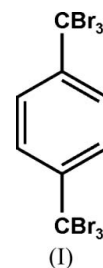
The title compound, C₈H₄Br₆, (I), initially crystallized from deuteriochloroform as the concomitant polymorphs (Ia) (prisms, space group *P2₁/n*, *Z* = 2) and (Ib) (hexagonal plates, space group *C2/c*, *Z* = 4). The molecules in both forms display crystallographic inversion symmetry. All further attempts to crystallize the compound led exclusively to (Ib), so that (Ia) may be regarded as a 'disappearing polymorph'. Surprisingly, however, the density of (Ia) is greater than that of (Ib). The only significant difference between the molecular structures is the orientation of the CBr₃ groups. The molecular packing of both structures is largely determined by Br⋯Br interactions, although (Ia) also displays a C—H⋯Br hydrogen bond and both polymorphs display one Br⋯π contact. For (Ia), six of the eight contacts combine to form a tube-like substructure parallel to the *a* axis. For (Ib), the two shortest Br⋯Br contacts link 'half' molecules consisting of C—CBr₃ groups to form double layers parallel to (001) in the regions $z \approx \frac{1}{4}, \frac{3}{4}$.

Comment

We are interested in secondary interactions in brominated aromatic hydrocarbons [see, for example, our studies of all ten isomers of di(bromomethyl)naphthalenes; Jones & Kuś (2010), and references therein]. Such interactions may include 'weak' C—H⋯Br hydrogen bonds, Br⋯Br halogen bonds, π–π stacking, and H⋯π and Br⋯π contacts. We are currently preparing a study of several benzene derivatives multiply substituted with bromo, methyl and bromomethyl groups (Jones & Kuś, 2011). The title compound, 1,4-bis(tribromomethyl)benzene, (I), as a tribromomethyl derivative, is loosely related to these.

Single crystals of compound (I) were originally obtained when a deuteriochloroform solution of (I) in an NMR tube was allowed to evaporate. The sample consisted mostly of

colourless prisms, which when examined with polarized light proved to be twinned lengthwise. Larger crystals (up to 2 mm in length) were difficult to cut and, even ignoring the problems of twinning and absorption, tended to be of low quality, but eventually we succeeded in cutting a small crystal lengthwise to provide a single-crystalline fragment of usable quality. This is polymorph (Ia) (space group *P2₁/n*). A few thin hexagonal plates were also observed. One of these was investigated and proved to be a second polymorph, (Ib) (space group *C2/c*). The crystals used for X-ray measurements are shown in Fig. 1.



The molecules in both polymorphs crystallize with imposed inversion symmetry (Figs. 2 and 3). The main difference is in the orientation of the CBr₃ group; in (Ia), one Br atom (Br3) lies approximately in the ring plane, whereas for (Ib) this is not the case (Tables 1 and 3).

Clearly, the major structural interest centres on the molecular packing. Not surprisingly for a compound for which 60% of the terminal atoms are bromine, Br⋯Br interactions (Tables 2 and 4) dominate, at least numerically. Polymorph (Ia) has eight independent interactions of this type <3.99 Å, with the next longest at 4.14 Å, while (Ib) has seven (entries 4 and 5 are symmetry-equivalent) <4.08 Å, with the next longest at 4.23 Å. Additionally, (Ia) has one 'weak' hydrogen bond [H3⋯Br3ⁱ = 3.00 Å; symmetry code: (i) $x - 1, y, z$] and a Br⋯π interaction Br3⋯Cgⁱⁱ = 3.518 Å [Cg is the centroid of the aromatic ring; individual Br⋯Cⁱⁱ distances = 3.738 (2)–3.779 (2) Å and C—Br⋯Cgⁱⁱ = 115°; symmetry code: (ii) $-x + \frac{3}{2}, y + \frac{1}{2}, -z + \frac{1}{2}$]. Polymorph (Ib) has a Br⋯π interaction Br1⋯Cgⁱⁱⁱ = 3.503 Å [individual Br⋯Cⁱⁱⁱ distances = 3.473 (4)–3.702 (5) Å and C—Br⋯Cgⁱⁱⁱ = 153°; symmetry code: (iii) $x - \frac{1}{2}, y + \frac{1}{2}, z$].

It is not a trivial problem to decide when a Br⋯Br contact corresponds to a significant interaction. The shortest such contacts are *ca* 3.1–3.2 Å and tend to be observed in charge-assisted systems such as [Ph₃PSBr]⁺[AuBr₄]⁻ [3.151 (1) Å;

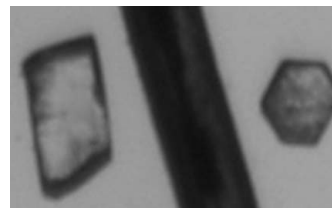
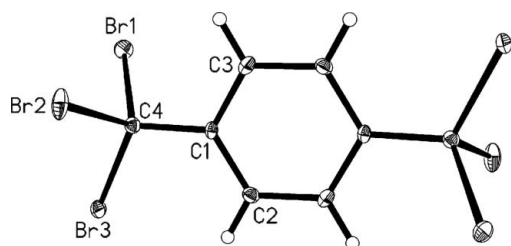
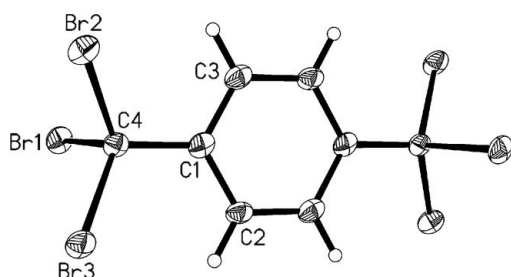


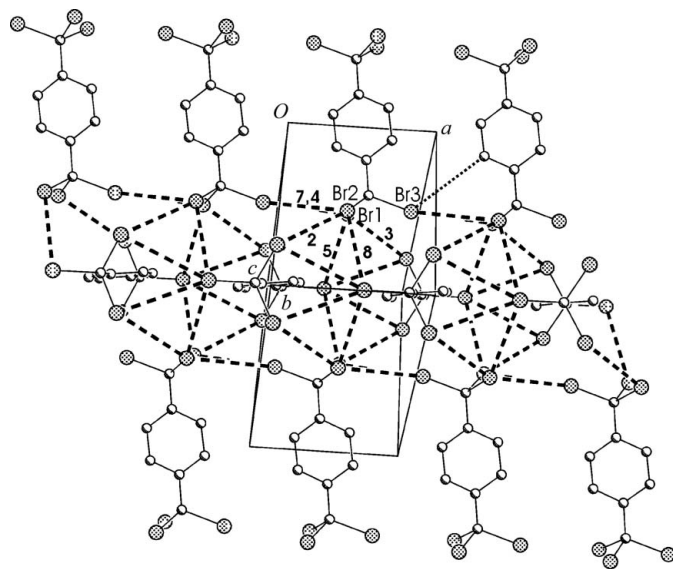
Figure 1
The measured crystals of polymorphs (Ia) (left) and (Ib) (right), compared with a human hair (centre; diameter *ca* 0.05 mm).


Figure 2

The molecule of polymorph (Ia), showing the atom-numbering scheme. Displacement ellipsoids are drawn at the 50% probability level. Only the asymmetric unit is numbered; unlabelled atoms are related by the symmetry operation $(-x + 1, -y, -z)$.

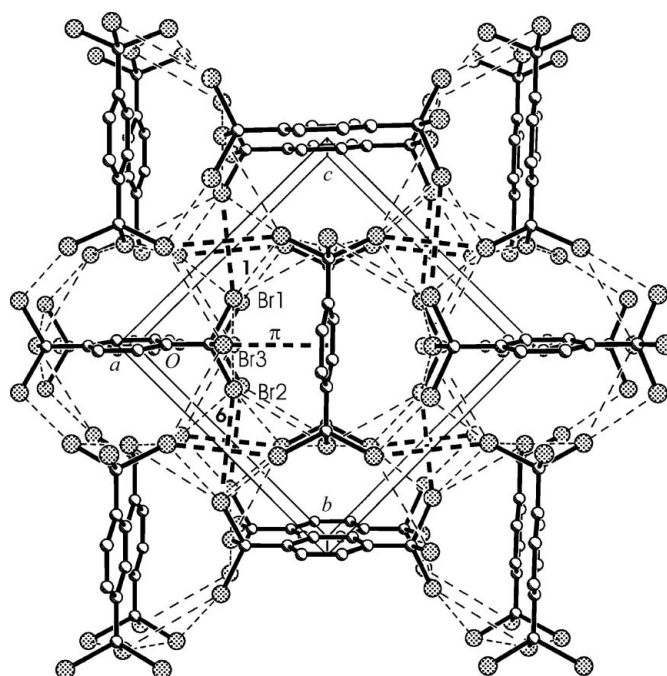

Figure 3

The molecule of polymorph (Ib), showing the atom-numbering scheme. Displacement ellipsoids are drawn at the 50% probability level. Only the asymmetric unit is numbered; unlabelled atoms are related by the symmetry operation $(-x + 1, -y + 1, -z + 1)$.


Figure 4

A packing diagram for polymorph (Ia), viewed perpendicular to $(01\bar{1})$. H atoms have been omitted. Br...Br interactions are indicated by dashed lines and are numbered according to Table 2; contact 4 lies behind contact 7. One representative C...Br interaction is represented by a dotted line (top right). Labelled Br atoms belong to the asymmetric unit and Br1 lies behind Br2.

Taouss & Jones, 2011]. ‘Spoke’ structures such as Ph_3PBr_2 , originally interpreted by the authors (Bricklebank *et al.*, 1992) as involving a long covalent Br—Br bond of 3.123 (2) Å, may also perhaps be interpreted as at least partly ionic [$\text{Ph}_3\text{PBr}^+\text{Br}^-$]. At the other extreme are contacts of ca 4 Å,


Figure 5

A packing diagram for polymorph (Ia), viewed parallel to the a axis. H atoms have been omitted. Br...Br interactions indicated by thin dashed lines correspond to those shown in Fig. 4, while those indicated by thick dashed lines and numbered (1 and 6) do not appear in Fig. 4. One representative Br... π interaction is represented by ‘ π ’. Labelled Br atoms belong to the asymmetric unit and the labels refer to atoms nearer the viewer.

which are significantly longer than twice the van der Waals radius (3.7 Å; Bondi, 1964) but may lead to striking patterns that are at the very least useful in describing molecular aggregates. We have described such long contacts as ‘tertiary interactions’ (du Mont *et al.*, 2008). Pedireddi *et al.* (1994) defined two categories of halogen–halogen contact in terms of the two C—Hal...Hal angles θ ; type II contacts tend to have $\theta_1 \simeq 90^\circ$ and $\theta_2 \simeq 180^\circ$ (or *vice versa*), whereas for type I contacts $\theta_1 \simeq \theta_2$. The former type may correspond better to significant interactions, consistent with the theoretical model of a region of positive charge in the extension of the C—Hal vector, whereas the latter type may correspond better to ‘chance’ contacts not indicating significant interactions. However, any inspection of systems with halogen–halogen contacts will reveal many cases not entirely consistent with the two standard types (*e.g.* short contacts with approximately equal angles; *cf.* Tables 2 and 4).

Polymorph (Ia) has only one Br...Br contact < 3.7 Å (entry 1 in Table 2), and despite its shortness this is a type I interaction with $\theta_1 = \theta_2$ by symmetry; all seven other contacts lie in the range 3.8–4.0 Å. Six of the eight contacts combine to form a tube-like substructure (Fig. 4) parallel to the a axis. A view of the structure parallel to the a axis (Fig. 5) shows that the tubes are connected by the two contacts $\text{Br1}\cdots\text{Br1}(-x + 1, -y, -z + 1)$ and $\text{Br2}\cdots\text{Br2}(-x + 1, -y + 1, -z)$ (entries 1 and 6 in Table 2), which are topologically closely similar but represent the shortest and longest contacts, respectively. This is a further reminder that the lengths of secondary or tertiary interactions

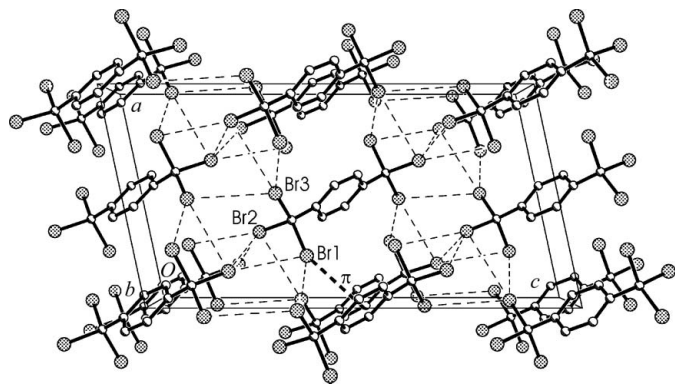


Figure 6

A packing diagram for polymorph (*Ib*), viewed parallel to the *b* axis. H atoms have been omitted. Br...Br interactions <4 Å are indicated by thin dashed lines. One representative Br... π interaction is represented by ' π '. Labelled Br atoms belong to the asymmetric unit.

may not be closely correlated with their (subjective) structural relevance.

The overall packing diagram of polymorph (*Ib*) is shown in Fig. 6. The Br...Br interactions can be seen in the regions $z \simeq \frac{1}{4}, \frac{3}{4}$. Two Br...Br contacts <3.7 Å (Table 4, entries 1 and 2) are appreciably shorter than all the others, and both correspond reasonably well to the type II criteria. To display the region at $z \simeq \frac{1}{4}$ more clearly, it is convenient to use only 'half' molecules consisting of C—CBr₃ groups, which are linked to form double layers, and to display only the two shortest Br...Br contacts (Fig. 7). Each individual layer is formed *via* contact No. 1 (these contacts run diagonally in the figure) and

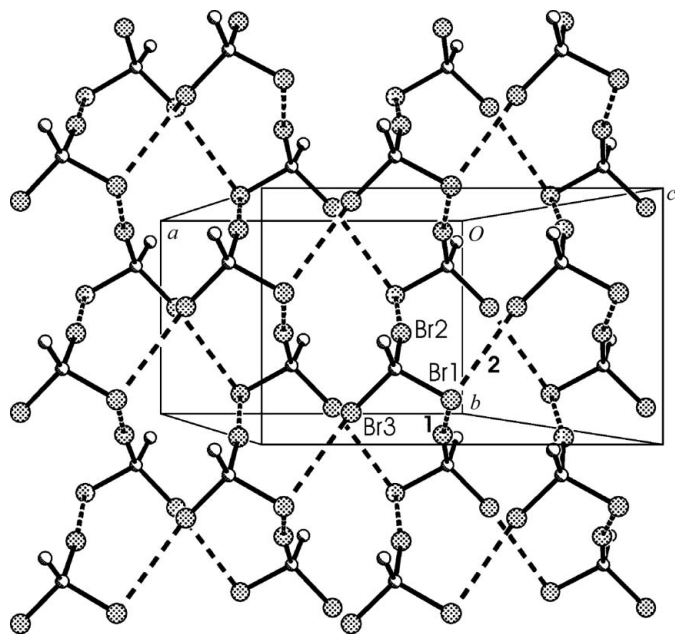


Figure 7

A packing diagram for polymorph (*Ib*), viewed perpendicular to (001), in the region $z \simeq \frac{1}{4}$. H atoms have been omitted and the molecules are 'halved' to C—CBr₃ groups. The two shortest Br...Br interactions are indicated by thick dashed lines and numbered according to the sequence of entries in Table 4. Labelled Br atoms belong to the asymmetric unit.

the layers are linked by contact No. 2 (almost perpendicular to the paper). Including all the interactions gives an impression of their density, but the resulting diagram is otherwise too complicated to interpret.

It seemed worthwhile to examine the relationship and possible interconversions between the two polymorphs. The original sample was no longer available and all further attempts at recrystallization led only to polymorph (*Ib*), as shown by powder diffractometry; measured and calculated [for (*Ib*)] powder patterns were essentially identical. Differential scanning calorimetry (DSC) measurements gave only a peak at the melting point (462.2 K). Melted and resolidified samples were amorphous, presumably because of decomposition (supported by DSC measurements, which showed a very broad melting peak for resolidified samples). Rapid evaporation from dichloromethane, slow evaporation from chloroform or stirring the solid with a saturated chloroform solution for a week all resulted in samples consisting only of (*Ib*). It seems, therefore, that (*Ib*) is the thermodynamically stable form at room temperature and that form (*Ia*) is a 'disappearing polymorph' (Dunitz & Bernstein, 1995). Curiously, the crystallographic density of (*Ia*) (3.165 Mg m⁻³) is greater than that of (*Ib*) (3.080 Mg m⁻³), which would not be expected if the predominance of (*Ib*) were attributable to more efficient packing.

Experimental

1,4-Bis(dibromomethylene)cyclohexane (0.50 g, 1.179 mmol) (Neidlein & Winter, 1998; *cf.* Hopf *et al.*, 2002) was dissolved in carbon tetrachloride (25 ml) under nitrogen. *N*-Bromosuccinimide (0.84 g, 4.716 mmol, 4 equivalents) and azobis(isobutyronitrile) (AIBN; 0.01 g; each 0.1 mol NBS requires 0.2 g AIBN) were added to the solution. The mixture was stirred for 1.5 h under reflux then allowed to cool to room temperature. The progress of the reaction was monitored by thin-layer chromatography (silica gel) with pentane. Purification by flash chromatography with pentane gave the pure product (yield 0.49 g, 72%; colourless crystals, m.p. 461–462 K). ¹H NMR (400 MHz, CDCl₃): δ 8.0 (s, 4H, arom.); ¹³C NMR (100 MHz, CDCl₃): δ 33.7 (s, CBr₃), 126.3 (*d*, arom. CH), 148.0 (s, arom. C); IR (film, ν , cm⁻¹): 3087 (*w*), 2923 (*w*), 2778 (*w*), 1490 (*w*), 1398 (*m*), 1181 (*m*), 1013 (*w*), 841 (*w*), 809 (*s*), 715 (*vs*), 682 (*m*), 647 (*vs, br*); EI-MS (*m/z*; relative intensity, %): 579.4 (2) [*M*⁸¹Br⁷⁹Br₃]⁺, 498.5 (14) [*M*⁸¹Br₂⁷⁹Br₃]⁺, 419.6 (100) [*M*⁸¹Br₂⁷⁹Br₂]⁺, 338.7 (10) [*M*⁸¹Br⁷⁹Br₂]⁺, 259.8 (65) [*M*⁸¹Br⁷⁹Br]⁺, 178.9 (22) [*M*⁷⁹Br]⁺, 100.0 (32), 74.0 (32), 50.0 (26). Elemental analysis calculated for C₈H₄Br₆: C 16.58, H 0.70, Br 82.72%; found: C 16.63, H 0.57, Br 82.22%. For an alternative preparation of the hexabromide from *p*-xylene, see Mataka *et al.* (1994).

Polymorph (*Ia*)

Crystal data

C ₈ H ₄ Br ₆	$V = 608.19 (5) \text{ \AA}^3$
$M_r = 579.57$	$Z = 2$
Monoclinic, $P2_1/n$	Mo $K\alpha$ radiation
$a = 6.3150 (3) \text{ \AA}$	$\mu = 19.76 \text{ mm}^{-1}$
$b = 9.8178 (4) \text{ \AA}$	$T = 100 \text{ K}$
$c = 9.8398 (4) \text{ \AA}$	$0.08 \times 0.06 \times 0.03 \text{ mm}$
$\beta = 94.486 (4)^\circ$	

Table 1

Selected torsion angles (°) for polymorph (Ia).

C2—C1—C4—Br3	−8.3 (2)	C3—C1—C4—Br1	51.5 (2)
C3—C1—C4—Br3	172.88 (14)	C2—C1—C4—Br2	111.73 (18)
C2—C1—C4—Br1	−129.69 (17)	C3—C1—C4—Br2	−67.09 (19)

Table 2

Br⋯Br contacts in polymorph (Ia) (Å, °).

C—Br⋯Br ^j —C ^j system	Br⋯Br ^j	C—Br⋯Br ^j angles	Symmetry operator <i>j</i>
1 C4—Br1⋯Br1—C4	3.6979 (4)	139.63 (6), 139.63 (6)	− <i>x</i> + 1, − <i>y</i> , − <i>z</i> + 1
2 C4—Br1⋯Br2—C4	3.8427 (3)	115.18 (6), 158.59 (6)	− <i>x</i> + $\frac{1}{2}$, <i>y</i> − $\frac{1}{2}$, − <i>z</i> + $\frac{1}{2}$
3 C4—Br1⋯Br2—C4	3.8354 (3)	107.96 (6), 117.67 (6)	<i>x</i> + $\frac{1}{2}$, − <i>y</i> + $\frac{1}{2}$, <i>z</i> + $\frac{1}{2}$
4 C4—Br1⋯Br3—C4	3.9750 (3)	92.15 (6), 152.00 (6)	<i>x</i> − 1, <i>y</i> , <i>z</i>
5 C4—Br1⋯Br3—C4	3.8573 (3)	145.15 (6), 94.69 (6)	<i>x</i> − $\frac{1}{2}$, − <i>y</i> + $\frac{1}{2}$, <i>z</i> + $\frac{1}{2}$
6 C4—Br2⋯Br2—C4	3.9819 (5)	130.68 (6), 130.68 (6)	− <i>x</i> + 1, − <i>y</i> + 1, − <i>z</i>
7 C4—Br2⋯Br3—C4	3.9288 (3)	93.53 (6), 153.70 (6)	<i>x</i> − 1, <i>y</i> , <i>z</i>
8 C4—Br2⋯Br3—C4	3.8815 (3)	129.46 (6), 93.57 (6)	− <i>x</i> + $\frac{3}{2}$, <i>y</i> + $\frac{1}{2}$, − <i>z</i> + $\frac{1}{2}$

Table 3

Selected torsion angles (°) for polymorph (Ib).

C3—C1—C4—Br2	−35.3 (5)	C2—C1—C4—Br3	29.1 (5)
C2—C1—C4—Br2	150.3 (4)	C3—C1—C4—Br1	84.6 (5)
C3—C1—C4—Br3	−156.5 (4)	C2—C1—C4—Br1	−89.8 (4)

Data collection

Oxford Xcalibur Eos diffractometer
Absorption correction: multi-scan
(*CrysAlis PRO*; Oxford
Diffraction, 2009)
*T*_{min} = 0.554, *T*_{max} = 1.000

15682 measured reflections
1795 independent reflections
1449 reflections with *I* > 2σ(*I*)
*R*_{int} = 0.033

Refinement

R[*F*² > 2σ(*F*²)] = 0.015
wR(*F*²) = 0.026
S = 0.86
1795 reflections

64 parameters
H-atom parameters constrained
Δ*ρ*_{max} = 0.53 e Å^{−3}
Δ*ρ*_{min} = −0.53 e Å^{−3}

Polymorph (Ib)

Crystal data

C₈H₄Br₆
*M*_r = 579.57
Monoclinic, *C*2/*c*
a = 10.1640 (9) Å
b = 6.5048 (7) Å
c = 19.3410 (17) Å
β = 102.152 (9)°

V = 1250.1 (2) Å³
Z = 4
Cu Kα radiation
μ = 22.89 mm^{−1}
T = 103 K
0.04 × 0.04 × 0.02 mm

Data collection

Oxford Xcalibur Nova Atlas
diffractometer
Absorption correction: multi-scan
CrysAlis PRO (Oxford
Diffraction, 2009)
*T*_{min} = 0.439, *T*_{max} = 1.000

7801 measured reflections
1271 independent reflections
1163 reflections with *I* > 2σ(*I*)
*R*_{int} = 0.076

Table 4

Br⋯Br contacts in polymorph (Ib) (Å, °).

C—Br⋯Br ^j —C ^j system	Br⋯Br ^j	C—Br⋯Br ^j angles	Symmetry operator <i>j</i>
1 C4—Br1⋯Br2—C4	3.6912 (7)	87.83 (12), 163.67 (13)	− <i>x</i> + $\frac{1}{2}$, <i>y</i> + $\frac{1}{2}$, − <i>z</i> + $\frac{1}{2}$
2 C4—Br1⋯Br3—C4	3.5799 (8)	94.47 (14), 154.20 (12)	<i>x</i> − $\frac{1}{2}$, <i>y</i> − $\frac{1}{2}$, <i>z</i>
3 C4—Br2⋯Br2—C4	4.0094 (10)	101.61 (12), 101.61 (12)	− <i>x</i> + 1, <i>y</i> , − <i>z</i> + $\frac{1}{2}$
4 C4—Br2⋯Br2—C4	3.8353 (6)	146.53 (13), 84.08 (14)	− <i>x</i> + $\frac{1}{2}$, <i>y</i> − $\frac{1}{2}$, − <i>z</i> + $\frac{1}{2}$
5 C4—Br2⋯Br2—C4	3.8353 (6)	84.08 (14), 146.53 (13)	− <i>x</i> + $\frac{1}{2}$, <i>y</i> + $\frac{1}{2}$, − <i>z</i> + $\frac{1}{2}$
6 C4—Br2⋯Br3—C4	3.8068 (7)	88.14 (12), 148.31 (13)	<i>x</i> − $\frac{1}{2}$, <i>y</i> − $\frac{1}{2}$, <i>z</i>
7 C4—Br2⋯Br3—C3	4.0730 (8)	138.09 (12), 77.51 (13)	− <i>x</i> + $\frac{1}{2}$, <i>y</i> − $\frac{1}{2}$, − <i>z</i> + $\frac{1}{2}$
8 C4—Br3⋯Br3—C4	3.9507 (10)	107.85 (12), 107.85 (12)	− <i>x</i> + 1, <i>y</i> , − <i>z</i> + $\frac{1}{2}$

Refinement

R[*F*² > 2σ(*F*²)] = 0.037
wR(*F*²) = 0.103
S = 1.05
1271 reflections

64 parameters
H-atom parameters constrained
Δ*ρ*_{max} = 1.02 e Å^{−3}
Δ*ρ*_{min} = −0.93 e Å^{−3}

For polymorph (Ib), 34 reflections at high angle with *F*_o << *F*_c were omitted from the refinement. It is not clear whether these errors were caused by hardware or software problems, or by any imperfection of the crystal. H atoms were introduced at calculated positions and refined using a riding model, with C—H = 0.95 Å and *U*_{iso}(H) = 1.2*U*_{eq}(C).

For both polymorphs, data collection: *CrysAlis PRO* (Oxford Diffraction, 2009); cell refinement: *CrysAlis PRO*; data reduction: *CrysAlis PRO*; program(s) used to solve structure: *SHELXS97* (Sheldrick, 2008); program(s) used to refine structure: *SHELXL97* (Sheldrick, 2008); molecular graphics: *XP* (Siemens, 1994); software used to prepare material for publication: *SHELXL97*.

Supplementary data for this paper are available from the IUCr electronic archives (Reference: FA3260). Services for accessing these data are described at the back of the journal.

References

Bondi, A. (1964). *J. Phys. Chem.* **68**, 441–451.
Bricklebank, N., Godfrey, S. M., Mackie, A. G., McAuliffe, C. A. & Pritchard, R. G. (1992). *J. Chem. Soc. Chem. Commun.* pp. 355–356.
Dunitz, J. D. & Bernstein, J. (1995). *Acc. Chem. Res.* **28**, 193–200.
Hopf, H., Kämpen, J., Bubenitschek, P. & Jones, P. G. (2002). *Eur. J. Org. Chem.* pp. 1708–1721.
Jones, P. G. & Kuš, P. (2010). *Z. Naturforsch. Teil B*, **65**, 433–444.
Jones, P. G. & Kuš, P. (2011). *Z. Naturforsch. Teil B*, **66**. In preparation.
Mataka, S., Liu, G.-B., Sawada, T., Kurisu, M. & Tashiro, M. (1994). *Bull. Chem. Soc. Jpn.*, **67**, 1113–1119.
Mont, W.-W. du, Bätcher, M., Daniliuc, C., Devillanova, F. A., Druckenbrodt, C., Jeske, J., Jones, P. G., Lippolis, V., Ruthe, F. & Seppälä, E. (2008). *Eur. J. Inorg. Chem.* pp. 4562–4577.
Neidlein, R. & Winter, M. (1998). *Synthesis*, pp. 1362–1366.
Oxford Diffraction (2009). *CrysAlis PRO*. Version 1.171.33.40. Oxford Diffraction Ltd, Yarnton, Oxfordshire, England.
Pedireddi, V. R., Reddy, D. S., Goud, B. S., Craig, D. C., Rae, A. D. & Desiraju, G. R. (1994). *J. Chem. Soc. Perkin Trans. 2*, pp. 2353–2360.
Sheldrick, G. M. (2008). *Acta Cryst. A* **64**, 112–122.
Siemens (1994). *XP*. Siemens Analytical X-ray Instruments Inc., Madison, Wisconsin, USA.
Taouss, C. & Jones, P. G. (2011). *Dalton Trans.* **40**. In the press.